Carbohydrate Polymers 110 (2014) 423–429

Contents lists available at ScienceDirect

Carbohydrate Polymers

journal homepage: www.elsevier.com/locate/carbpol

Characterization of new natural cellulosic fiber from *Cissus quadrangularis* root

S. Indran [a], R. Edwin Raj [a,*], V.S. Sreenivasan [b]

[a] Department of Mechanical Engineering, St. Xavier's Catholic College of Engineering, Nagercoil 629003, India
[b] Department of Mechanical Engineering, VV College of Engineering, Tisaiyanvilai 627657, India

ARTICLE INFO

Article history:
Received 24 February 2014
Received in revised form 4 April 2014
Accepted 17 April 2014
Available online 26 April 2014

Keywords:
Cissus quadrangularis
Cellulosic fiber
XRD
FTIR
SEM
TGA

ABSTRACT

Fiber reinforced polymer composites are replacing many metallic structures due to its high specific strength and modulus. However commonly used man-made E-glass fibers are hazardous for health and carcinogenic by nature. Comprehensive characterization of *Cissus quadrangularis* root fiber such as anatomical study, chemical analysis, physical analysis, FTIR, XRD, SEM analysis and thermo gravimetric analysis are done. The results are very encouraging for its application in fiber industries, composite manufacturing, etc. Due to its light weight and the presence of high cellulose content (77.17%) with very little wax (0.14%) provide high specific strength and good bonding properties. The flaky honeycomb outer surface and low microfibril angle revealed through electron microscopy contributes for its high modulus. The thermo gravimetric analysis indicates better thermal stability of the fiber up to 230 °C, which is well within the polymerization process temperature.

1. Introduction

Most of the fiber reinforced polymer composite material (FRP) consists of a polymer matrix with man-made vitreous fibers (MMVFs) like glass wool, carbon, aramid, rock wool, etc. However, most of them are carcinogenic in nature (Cavallo et al., 2004). The increasing risk of cancer to long term exposure of MMVFs was investigated and reported (Zhong, Ong, & Whong, 1997). Researchers are in search of better alternatives to MMVFs, especially to commonly used glass fiber for general applications. Nature always comes in handy for every good alternative materials search. There are some good fiber yielding plants which are cost effective without compromising mechanical properties (Sreenivasan, Somasundaram, Ravindran, Manikandan, & Narayanasamy, 2011). The fibers can be extracted from different parts of the plant such as stem, leaf, petioles, roots, fruits and seeds. Moreover, only a few species can contribute both as a source of fiber and for medical applications. In general, natural fibers are harmless, renewable, biodegradable and cost effective with high specific strength in comparison with synthetic fiber.

Cissus quadrangularis (CQ) is one such plant, which is mostly available in the tropical regions of India with both medicinal value and rich fiber content in its roots as well as in stem. CQ is probably native to India or Srilanka, but is also found in Africa, Arabia, and South Asia. Till date there are only little research work on the fibers extracted from this plant. CQ belongs to the family *Vitaceae* and its botanical name is *Vitis quadrangularis*/*C. quadrangularis* (Anitha & Suji, 2012). CQ is a common perennial climber reaching a height of around 2.5 m and has quadrangular sectioned branches with internodes of 1.5–1.8 cm width and 10–15 cm long (Fig. 1). Their roots are very easy to extract as they will not penetrate very deep, with maximum penetration of around 1 m.

CQ can be used as a medicine for hemorrhoid (Sapsrithong, Kaewprem, Tongumpai, Nusuetrong, & Meksuriyen, 2012), fatty liver disease (Jeya & Anuratha, 2010), asthma, indigestion, ear diseases, irregular menstruation, skin diseases (Bhujade et al., 2012), gas trouble (Mallika & Shyamala Devi, 2006; Mariana de Paula Ferreira et al., 2008), neutrophil mediated tissue injury protection, diabetes, scurvy, peptic ulcer disease (PUD), Malaria (Mallika & Shyamala Devi, 2006), etc. In this paper, the *C. quadrangularis* root fiber (CQRF) is taken for investigation and compared with other known natural cellulosic fibers. To the best of the reference from literature, extensive CQRF characterization is done for the first time in this paper. CQRF was examined

* Corresponding author. Tel.: +91 09442054535; fax: +91 04652 233982.
E-mail addresses: redwinraj@gmail.com, r_edwinraj@yahoo.co.uk (R. Edwin Raj).

http://dx.doi.org/10.1016/j.carbpol.2014.04.051
0144-8617/

Fig. 1. *Cissus quadrangularis* plant with its extracted root fiber.

to determine the anatomy, chemical, mechanical and thermal properties.

2. Materials and methods

2.1. Extraction procedure for root fiber

The CQ roots were collected from farms around the village called Asarivilai in Kanyakumari District, Tamil Nadu, India, and extracted using microbial degradation technique (Saravanakumar, Kumaravel, Nagarajan, Sudhakar, & Baskaran, 2013). After removing the dirt and other foreign materials, the roots were immersed in water for two weeks to allow microbial degradation. They were then taken out and thoroughly washed with fresh water and dried in the sun light for a week to remove the moisture content. The soil particles and outer layer of the root where then removed by traditional combing process with metal teeth brush. The retained inner layer is a bundle of fiber which can be separated for further use.

2.2. Characterization of CQRF

2.2.1. Root anatomy

The segregated healthy root fibers were subjected to microstructural analysis for anatomical studies. The roots were cut into small pieces (10 mm × 10 mm) and immersed in FAA solution (5 ml formaldehyde + 5 ml acetic acid + 90 ml 70% ethyl alcohol) for 24 h for preserving the tissues. They were then dehydrated through a graded tertiary butyl alcohol series and embedded in paraffin (Sass, 1940). Microstructural specimens were prepared by sectioning them of 10–12 μm size using rotary microtome, then affixed to a glass slide and stained with a mixture of Toluidine blue, safraine, fast green and Lugo's iodine solution (O'Brien, Feder, & McCull, 1964) for clarity picture. Polarized light microscope unit (Nikon, Japan) was used for polarized light microscope histochemistry study.

2.2.2. Chemical analysis

By using standard test procedures, the cellulose, hemicellulose and lignin contents of CQRF was determined (Doree, 1950; Pearl, 1967). Liquid immersion test using toluene was carried out to measure the density (Beíakou, Ntenga, Lepetit, Ateíba, & Ayina, 2008) and the wax content was quantified as per the standard protocol (Conrad, 1944). The ash content was analyzed as per the ASTM E1755-61 standard (Reddy & Yang, 2008) and the sample was dried in an oven at 104 °C for 4 h to determine the moisture content (Sreenivasan et al., 2011). The chemical compositions of other natural cellulosic fibers were compared from the available data of various review articles and are tabulated in Table 1.

2.2.3. Physical property analysis

Tensile specimens were prepared from dried root fibers and subjected to tensile loading in an INSTRON universal testing machine (5500R) computerized with data acquisition system at different gauge lengths (GL) of 10, 20, 30, 40 and 50 mm. The tensile tests were conducted as per ASTM D3822-07 standard at a constant cross head speed of 0.1 mm/min. To rationalize the effect of variability of the natural fibers, 20 samples were tested at each GL, and the average values were recorded. All the testings' were conducted at

Table 1
Properties of CQRF in comparison with cellulose based natural fibers and Man-made synthetic fibers (Dittenber & Ganga Rao, 2012; Faruk, Bledzkia, Finkb, & Sain, 2012; Fernando Pacheco-Torgal & Jalali, 2011; Hejazi, Sheikhzadeh, Abtahi, & Zadhoush, 2012; Jawaid & Abdul Khalil, 2011; Koronis, Silva, & Fontul, 2013; Ku, Wang, Pattarachaiyakoop, & Trada, 2011; Mantia & Morreale, 2011; Ho et al., 2012; Sathishkumar, Navaneetha krishnan, & Shankar, 2012; Satyanarayana, Sukumaran, Mukherjee, Pavithran, & Pillai, 1990; Sreenivasan et al., 2011).

Fiber	Chemical properties					Physical properties			
	Cellulose (%)	Hemicellulose (%)	Lignin (%)	Wax (%)	Moisture (%)	Density (g/cm^3)	Elongation %	Tensile Strength (MPa)	Young's modulus (GPa)
CQRF	**77.17**	**11.02**	**10.45**	**0.14**	**7.3**	**1.51**	**3.57–8.37**	**1857–5330**	**68–203**
Cotton	82.7	5.7	–	–	1.0	1.6	7–8	400	5–12
Coir	32–43	0.15–0.25	40–45	–	–	1.2	30	593	4–6
Jute	64.4	12	11.8	0.7	1.1	1.3	1.5–1.8	393–773	26
Flax	64.1	16.7	2.0	1.5–3.3	3.9	1.5	2.7–3.2	500–1500	27
Hemp	68	15	10	0.8	–	1.47	2–4	690	70
Kenaf	31–72	20.3–21.5	8–19	–	–	1.45	1.6	930	53
Ramie	68.6–85	13–16.7	0.5–0.7	0.3	7.5–17	1.5	2–3	220–938	44–128
Sisal	60–78	10.0–14.2	8.0–14	2.0	10–22	1.5	2–2.5	511–635	9–22
Pineapple leaf	70–83	–	5–12.7	–	11.8	1.4	0.8–1	413–1627	34–82
Banana	56–63	20–25	7–9	3	–	1.35	1–3.5	529–759	8
Palmyrah	40–52	42–43	–	–	–	1.09	7–15	180–215	7–604
Bamboo	73.83	12.49	10.15	3.16	–	0.91	1.4	503	35.91
Sansevieriacylindrica	79.7	10.13	3.8	0.09	6.08	0.92	12.3–13.7	666–706	6–8
Curaua	70.7	9.9	7.5–11.1	–	–	1.4	3.7–4.3	500–1150	11
Bagasse	55.2	16.8	25.3	–	–	1.2	1.1	20–290	19–27
E-glass	–	–	–	–	–	2.5	0.5	2000–3500	70
Aramid (Std.)	–	–	–	–	–	1.4	3.3–3.7	3000–3150	63–67
Carbon (Std. PAN-based)	–	–	–	–	–	1.4	1.4–1.8	4000	230–240

Bold symbolizes the experimental result of the author, whereas the other data are collected from the published literature.

ambient temperature (28 °C) with a relative humidity of around 65%. The fineness of the CQRF was determined in terms of linear density in accordance with ASTM D 1577-07 (2012) standards. The linear density was obtained as Tex/Denier by weighing 100 single fibers with each measuring 90 mm in length.

2.2.4. FTIR analysis

Perkin Elmer Spectrum RXI Fourier Transform Infrared (FTIR) Spectrometer was used to derive the FTIR spectra of the CQRF in KBr matrix with a scan rate of 32 scans per minute at a resolution of 2 cm^{-1} in the wave number region 400–4000 cm^{-1}. The chopped samples were grounded to fine powder using a mortar and pestle and then mixed with KBr. They were then pelletized by applying pressure to prepare the specimen to record the FTIR spectra under standard conditions. FTIR spectra are used to determine the presence of free functional groups in CQRF.

2.2.5. XRD analysis

The powdered samples were subjected to X-ray diffraction in Rigaku X-ray diffractometer D/Max Ultima III with monochromatic Cu Kα radiation to determine the Crystallinity Index (*CI*) and crystallite size of the CQRF. The XRD analysis was carried out in (2θ) range of 10–80° with goniometer speed of 5°/min. The integrated intensities of the Bragg peaks in the spectrum of the CQRF was identified and their *CI* were estimated.

2.2.6. SEM analysis of the CQRF

The surface of CQRF was examined using a scanning electron microscope, HITACHI Model S3000H for observing the surface morphology. The specimens were coated with platinum layer to avoid electron beam charging effects during examination. The SEM studies were conducted with an electron beam accelerating potential of 3 kV.

2.2.7. TG–DTG analysis of the CQRF

The thermal stability behavior of the CQRF was assessed by Thermogravimetric (TG and DTG) analysis using Jupiter Simultaneous thermal analyzer (Model STA 449 F3, NETZSCH, Germany). To avoid oxidation effects the TGA analysis were carried out in nitrogen atmosphere at a flow rate of 20 ml/min. Ten milligram of the CQRF was crushed and kept in alumina crucible to avoid the temperature variations measured by the thermocouple. The heating rate is maintained at 10 °C/min for heating it from 28 °C to 1000 °C.

3. Results and discussion

3.1. Anatomy of CQRF

Well-developed matured CQ root with secondary growth was studied for its anatomical structure through optical microscope. The root structure shows a highly wavy periderm at the outer surface followed by epidermis and cortex, which is uneven in thickness. The inner portion of the root comprise of vascular cylinder and xylem masses (Fig. 2a). The periderm is superficial and forms highly folded ridges and furrows, which includes 3 or 4 layers of compressed narrow thick walled cells. The epidermis is more or less intact enclosing the ridge and furrow surface of the root. The cortex has *parenchymatous* and *secondary phloem* cortical cells. It consists of wide zone of parenchyma cells with dense tannin content, scattered sieve elements, calcium crystals of druses and raphides, which were not very distinct. Similarly, the druses are more in number than the raphide bundles and are scattered throughout the cortex (Fig. 2b and c). The druses are of 20 μm in diameter and the raphides are 20 μm × 60 μm in size. The xylem cylinder includes six radial segments of divided xylem masses. Each segment has

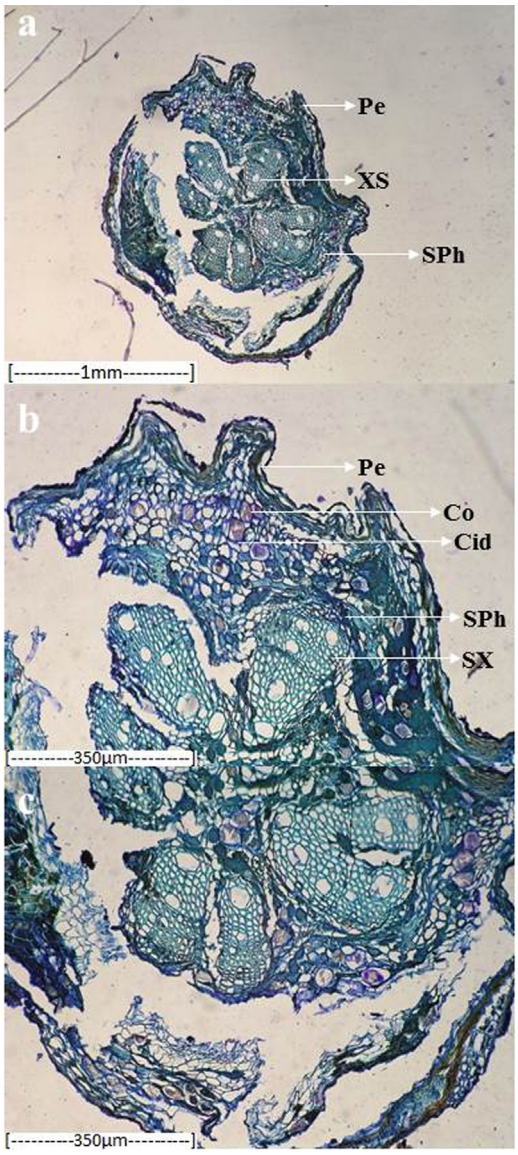

Fig. 2. Optical microscopic image of *Cissus quadrangularis* root in the transverse direction – (a) 10×, (b) 40× and (c) 40× (Pe, periderm; XS, xylem segment; Co, cortex; Cid, crystal bearing idioblast; SX, secondary xylem; SPh, secondary phloem).

few diffusely distributed vessel elements (approximately 30 μm in diameter) and wide *sclerenchymatous* ground tissue.

The fiber bundles were mostly observed in the ground tissue having honeycomb structure in the transverse section with small porosity (Fig. 2c). They are surrounded by secondary phloem and secondary xylem cells. The average diameter of fiber is in the range of 350–770 μm. The CQRF was extracted by natural degradation technique as decortication extraction method will damage the fiber structure (Sreenivasan et al., 2011). The extracted fibers were then examined in the polarized microscope to study its structure, which shows three distinct layers; the outer primary wall, followed by lignified wall and secondary wall and the cell lumen at the inner portion.

3.2. Chemical analysis of CQRF

The chemical composition of the natural fibers greatly influences the properties such as mechanical, fire resistant, resilience, and biodegradability. High cellulose content (77.17 wt.%) of CQRF has significantly contributed for the enhancement of mechanical

properties of this fiber (Baley, 2002). However, the hemicellulose content will reduce the strength of the fiber as it leads to degradation and disintegration of micro fibrils. The hemicellulose content of CQRF is only 11.02 wt.% (Morvan, Jauneau, Flaman, Millet, & Demarty, 1990). The presence of lignin (10.45 wt.%) will also influences the fiber structure, property and morphology (Mohanty, Misra, & Hinrichsen, 2000). The presence of wax content will reduce the interfacial bonding strength between the fiber and matrix in composite (Sreenivasan et al., 2011). The wax content of CQRF is only 0.14 wt.%, which is significantly low in comparison with flax, sisal, bamboo, etc. and may enhance bonding while making composite materials.

3.3. Physical properties of CQRF

Mechanical properties of the CQRF depend largely on the cell wall structure and the chemical composition, especially the cellulose percentage. Fibers were tested in the universal testing machine at five different gauge lengths (GL) to determine its mechanical properties. 20 samples were randomly selected from a given batch for each test conditions and the obtained results are tabulated in Table 2. The deviation from the mean values is quite large, which was expected for any natural fiber characterization. However, there is no significant variation in the tensile strength determined at different gauge lengths but it can be noted that as the gauge length increases the standard deviation decreases. The variation in young's modulus was rather high which may be due to artifacts. The average fiber diameters were determined from 30 samples through optical microscope images taken in the longitudinal direction using Image-pro software (Fig. 3a). They were also verified by the images taken at transverse direction using ImageJ software (Fig. 3b, Table 2). The physical properties of the CQRF fibers were compared with other natural and man-made fibers from the published literatures and are tabulated in Table 1. The physical properties, such as tensile strength and modulus are substantial enough for its usage as reinforcing material in composite manufacturing. The moderate density of the fiber in comparison with E-glass fiber contributes in achieving weight reduction for structural applications.

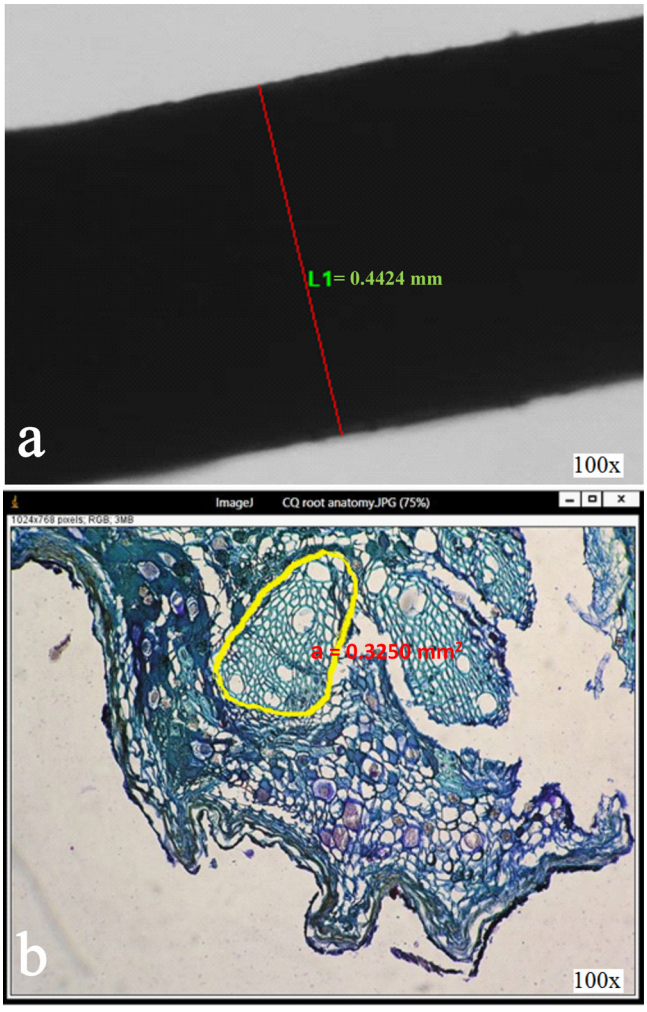

Fig. 3. Polarized microscopic images of CQRF for the determination of fiber diameter (a) using Image-pro software along the fiber longitudinal direction and (b) using ImageJ software at the transverse direction.

3.4. FTIR analysis

FTIR spectra show well-defined peaks of CQRF at 3333, 1600, 1419, 1316, 1024 and 775 cm^{-1} (Fig. 4). The peak at 3333 cm^{-1} belongs to the carboxylic acid O—H stretching due to the presence of cellulose I (Jayaramudu, Guduri, & Varada Rajulu, 2010) and the sp^3 C—H stretching occurred due to the vibration of cellulose, which is noted by a moderate peak at 2919 cm^{-1} (Kiruthika & Veluraja, 2009). A small peek at 1690 cm^{-1} is attributed to the presence of carboxyl stretching of C—O, which is an acetyl groups in hemicellulose. The smaller peak indicates less percentage content of hemicellulose, which is advantageous, because higher content will affect the mechanical properties of CQRF. The

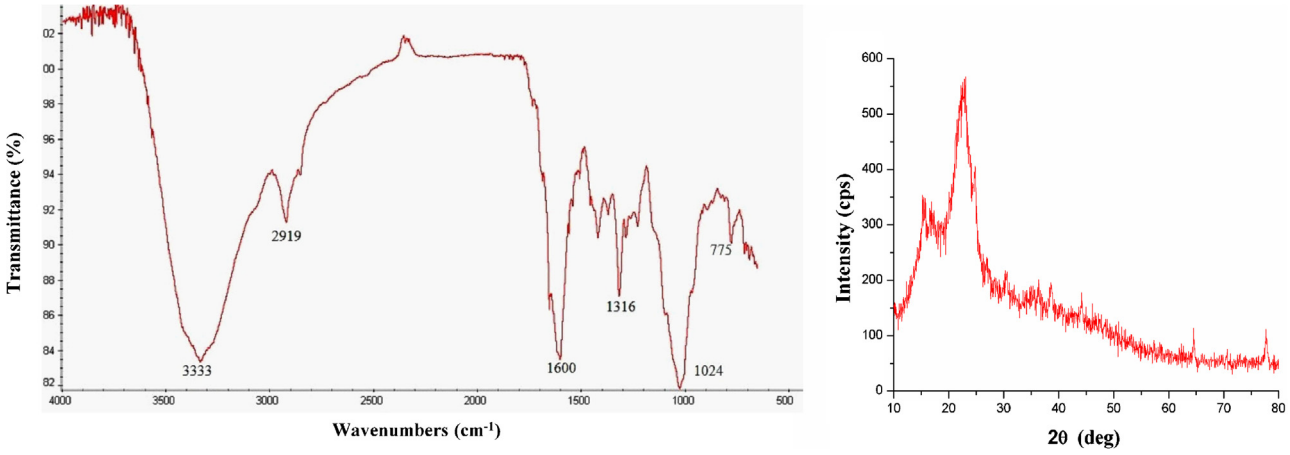

Fig. 4. FTIR and XRD spectrum of the CQRF.

peak at band 1600 cm^{-1} indicates the C=C aromatic stretching with strong conjugated C—C bond and this peak is attributed to lignin content in the fiber (Saravanakumar et al., 2013). Similarly, the peak at 1419 cm^{-1} band shows the C—H bending and 1316 cm^{-1} band is ascribed to strong acyl C—O with overlapped C—H stretching of phenols and esters. The band 1024 cm^{-1} corresponds to alkoxy C—O ordinary bond bending vibration (Kiruthika & Veluraja, 2009) and the smaller peak at 775 cm^{-1} represent the presence of saline content (Khan & Drzal, 2004). The natural fiber bands can vary by around ±16 cm^{-1} from their position for different studies (Zhbankov et al., 2002).

3.5. XRD analysis

Fig. 4 shows the emblematic X-ray diffraction spectrum for CQRFs. The first two peaks occurred at $2\theta = 15.5^\circ$ and $2\theta = 16.3^\circ$ are attributed to (2 0 0) crystallographic plane. The major peak at $2\theta = 22.55^\circ$ is attributed to (1 $\bar{1}$ 0) crystallographic plane (Reddy, & Yang, 2005). These peaks belong to cellulose type I, which is semi-crystalline in structure (Helbert, Sugiyma, Ishihara, & Yamanaka, 1997; Sreenivasan et al., 2011). In corroboration with chemical and FTIR analysis the XRD peak result confirms the presence of cellulose type I in CQRF.

The *CI* was calculated using the expression (1) as 56.6%. The *CI* was calculated using the expression (Segal, Creely, Martin, & Conrad, 1959; Sreenivasan et al., 2011):

$$CI = \frac{H_{22.55} - H_{18.5}}{H_{22.55}} \quad (1)$$

where $H_{22.5}$ is the height of the XRD peak at $2\theta = 22.55^\circ$; which contribute both amorphous and the crystalline fractions. $H_{18.5}$ is the small peak intensity height at $2\theta = 18.5^\circ$ and is attributed to the amorphous fraction. The calculated *CI* value higher than that of *Wrighitia tinctoria* seed fiber (49.2%) and smaller than ramie (58%), *Sansevieria cylindrica* leaf fibers (60%), *Raffia textilis* (64%), sisal (71%), jute (71%), flax (80%) and hemp (88%) (Sreenivasan et al., 2011). A higher value of CI indicates the fiber crystallites are orderly in nature. The crystallite size (L) was estimated using Scherrer's formula (D'Almeida, Aquino, & Monteiro, 2006; Elenga, Dirras, Goma Maniongui, Djemia, & Biget, 2009):

$$L = \frac{K\lambda}{\beta \cos\ \theta} \quad (2)$$

where $K = 0.89$ is Scherrer's constant, β is the peak's full-width half-maximum (FWHM) and λ is the wavelength of the radiation. The crystalline size was calculated as 28.05 nm for the first crystallographic plane (2 0 0) and that of the second crystallographic plane (1 $\bar{1}$ 0) is 7.04 nm. The crystallite size reported for some natural fibers are *Raffia textilis* (32 nm), ramie fibers (16 nm), cotton fibers (5.5 nm), corn stalk fibers (3.8 nm) and flax fibers (2.8 nm) (Reddy & Yang, 2005; Sreenivasan et al., 2011). The lower crystal size structure tends to absorb more water than the higher crystal size structures.

3.6. SEM analysis of CQRF

The surface morphology of the CQRF was examined in the longitudinal direction in the scanning electron microscopy at different magnification and it is shown in Fig. 5a–c. Flaky cell structures with small honeycomb voids were observed on one side of the fiber whereas the other side appears to be smooth, showing the presence of microfibril (Charlet, Eve, Jernot, Gomina, & Breard, 2009). The flaky rough outer structures of the fiber enhance the bonding strength of the fiber with matrix in polymer composite manufacturing. The microfibril angle was measured using ImageJ software from

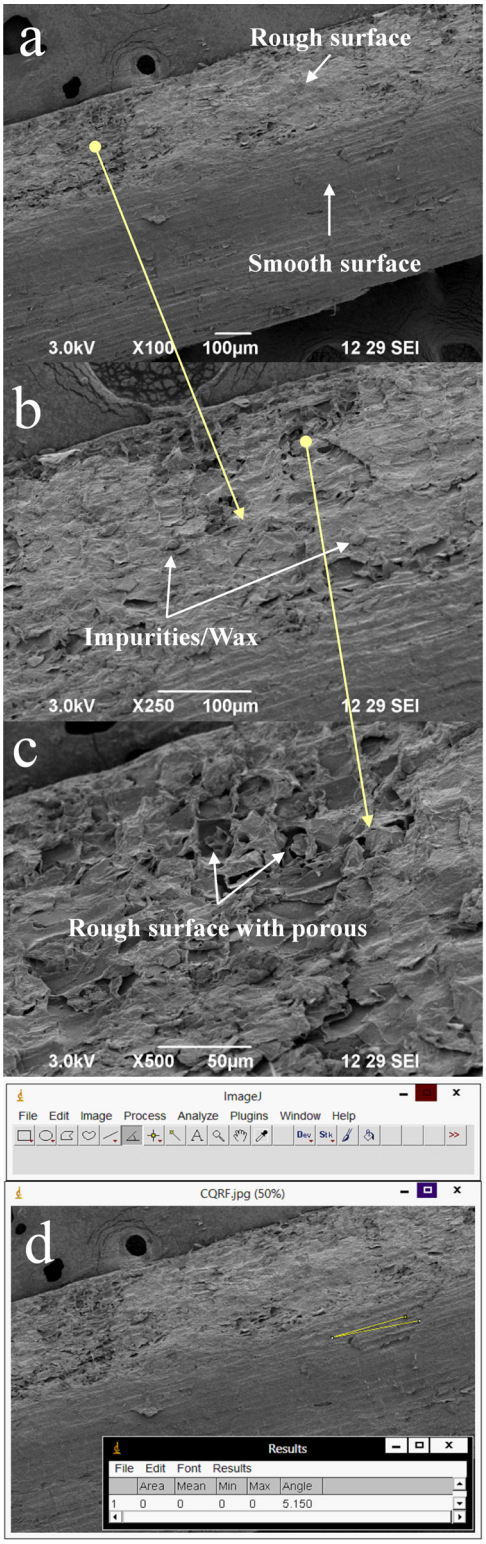

Fig. 5. Scanning electron micrographs of *Cissusquadrangularis* root – (a) 100×, (b) 250× and (c) 500×, (d) microfibril angle calculation using ImageJ software.

the SEM image as 5.15° (Fig. 5d). The microfibril angle (α) was also calculated using the global deformation equation as 5.89 ± 0.27°:

$$\varepsilon = \ln\left[1 + \frac{\Delta L}{L_o}\right] = -\ln(\cos\ \alpha) \quad (3)$$

where ε is the strain, α is the microfibril angle in degree, $[\Delta L/L_o]$ is the ratio of elongation. The reported microfibril angle for jute, flax,

Table 2
Mechanical properties of *Cissus quadrangularis* root fiber.

Gauge length (mm)	Tensile strength (MPa)	Young's modulus (GPa)	Strain to failure %	Cross sectional area (mm^2)
10	2516 ± 1052	91 ± 41	5.25 ± 4.21	0.3240 ± 0.2189
20	2817 ± 1209	93 ± 42	4.34 ± 3.12	0.3338 ± 0.1998
30	2860 ± 893	104 ± 41	4.33 ± 4.37	0.3424 ± 0.1526
40	2909 ± 915	132 ± 39	5.27 ± 4.74	0.3338 ± 0.1682
50	3172 ± 891	133 ± 36	4.93 ± 3.95	0.3364 ± 0.1192

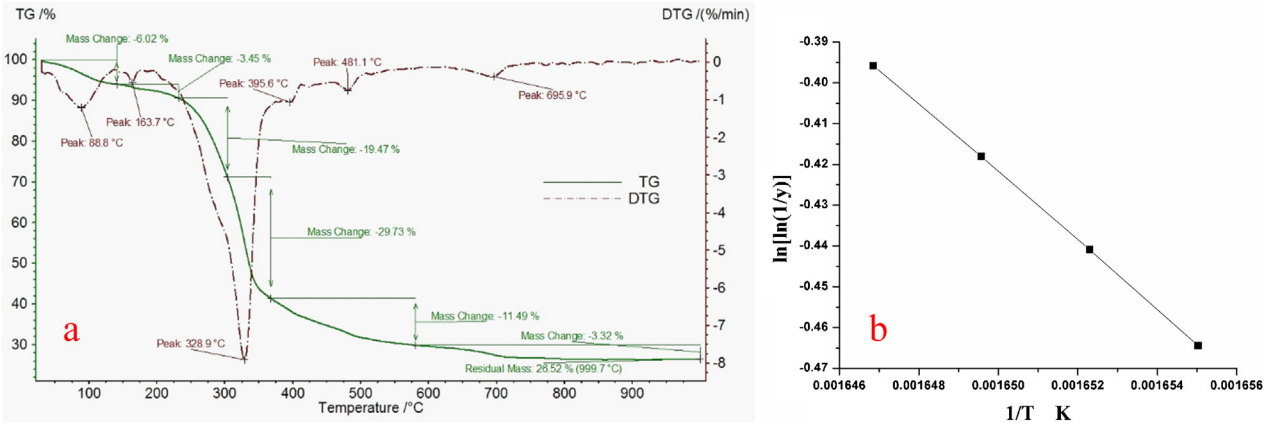

Fig. 6. Thermal analysis (a) TG and DTG curves of the CQRF, (b) Broido's Plot of the CQRF.

hemp, banana and *Prosopis juliflora* fibers are 8.1°, 5°, 6.2°, 11–12° and 10.64° respectively (Kulkarni, Satyanarayana, & Rohatgi, 1983; Perry, 1975; Saravanakumar et al., 2013).

3.7. Thermal analysis of the CQRF

The thermo gravimetric analysis (TGA) was done on CQRF to study its thermal stability. Fig. 6a shows a typical TGA and DTG curves of the CQRF powdered sample. The initial weight loss is reported at around 89 °C, which is attributed to the removal of moisture content from the fiber. The second minor dip is noted at around 163.7 °C, where CQRF suffered 9% degradation, where pyrolysis of lignin is initiated. Then CQRF was thermally stable up to around 230 °C, where no significant peak was observed. However, after 230 °C and up to 330 °C, a sudden dip can be noted in the DTG curve, indicating weight reduction which corresponds to the thermal decomposition of the hemicellulose and glycosidic links of cellulose (Azwa, Yousif, Manalo, & Karunasena, 2013). A noticeable peak at 328.9 °C shows the possible flinch of thermal decomposition of cellulose I and complete decomposition of α-cellulose respectively (Saravanakumar et al., 2013). Similar peaks were observed for bamboo, hemp, jute and kenaf fibers at 321 °C, 308.2 °C, 298.2 °C and 307.2 °C respectively (Yao, Wu, Lei, Guo, & Xu, 2008). Slow degradation of cellulose takes place at lower temperatures; whereas at high temperatures a rapid de-polymerization of cellulose molecules leading to cleavage of glycosyl units and the formation of levoglucosan (Cheng, Winter, & Stipanovic, 2012). Two small peaks were observed at 481 °C and 696 °C pertain to degradation and pyrolysis of lignin respectively (Azwa et al., 2013). At temperatures above 500 °C, the molecules break down into a variety of low molecular weight products, such as CO_2, CO, H_2O, hydrocarbons and hydrogen.

The apparent activation energy E_a was calculated to know the kinetic parameter of CQRF (Das & Chakrabarty, 2008) using the Broido's equation (4).

$$\varepsilon = \ln\left[\ln\left[\frac{1}{y}\right]\right] = -\left(\frac{E}{R}\right)\left[\left(\frac{1}{T}\right) + K\right] \quad (4)$$

where R is the universal gas constant (8.314 J/mol K), T is the temperature in Kelvin, y is the normalized weight (w_t/w_o), w_t symbolizes the weight of the sample at any time t, whereas w_o indicates the initial sample weight. The kinetic activation energy E_a = 74.18 kJ/mol was interpolated from the Broido's plot (Fig. 6b) of ln[ln(1/y)] verses (1/T) in Kelvin. The activation energy of CQRF is within the range specified for natural materials, i.e., 60–170 kJ/mol, which signifies that the CQRF fiber has thermal stability to withstand polymerization process temperature in polymer composite manufacturing (Di Blasi, 2002; Saravanakumar et al., 2013).

4. Conclusions

The characterization results obviously shows that the CQRF is a better alternate material for conventional man-made hazardous fibers because of its significant physical, mechanical and thermal degradation properties. The higher percentage of cellulose content (77.17 wt.%) and inconsequential presence of wax (0.14 wt.%) are notable properties for its usage as a reinforcing material in composite manufacturing. The density of CQRF is significantly lower (1.51 g/cm^3) in comparison with E-glass fiber (2.5 g/cm^3), whereas the mechanical properties are comparable with the conventional fibers. These combinations of properties provide high specific strength and specific modulus for its application in textiles and other structural applications. The SEM picture confirms the presence of microfibril with minimum angle between them, which contributes in providing higher strength, whereas the flaky cell surface provides good bonding characteristic with polymer matrix. The thermal analysis confirms the stability of CQRF up to 230 °C, which is well above the polymerization process temperature. These characterization results confirm its usage of CQRF for various industrial applications.

Acknowledgement

The first author acknowledges the Department of Science and Technology, Government of India for providing INSPIRE fellowship to carry out his research work.

References

Anitha, R., & Suji, P. (2012). Pharmacognostic evaluation of *Cissus quadrangularis* L. Stem. *International Journal of Pharmaceutical Sciences and Research*, *7*, 2296–2300.

Azwa, Z. N., Yousif, B. F., Manalo, A. C., & Karunasena, W. (2013). A review on the degradability of polymeric composites based on natural fibres. *Materials and Design*, *47*, 424–442.

Baley, C. (2002). Analysis of the flax fibers tensile behavior and analysis of the tensile stiffness increase. *Composites: Part A*, *33*, 939–948.

Beíakou, A., Ntenga, R., Lepetit, J., Ateíba, J. A., & Ayina, L. O. (2008). Physico-chemical and microstructural characterization of "Rhectophyllum camerunense" plant fiber. *Composites: Part A*, *39*, 67–74.

Bhujade, A. M., Talmale, S., Kumar, N., Gupta, G., Reddanna, P., Das, S. K., et al. (2012). Evaluation of *Cissus quadrangularis* extracts as an inhibitor of COX, 5-LOX, and pro inflammatory mediators. *Journal of Ethnopharmacology*, *141*, 989–996.

Cavallo, D., Campopiano, A., Cardinali, G., Casciardi, S., Simone, D. P., Kovacs, D., et al. (2004). Cytotoxic and oxidative effects induced by man-made vitreous fibers (MMVFs) in a human mesothelial cell line. *Toxicology*, *201*, 219–229.

Charlet, K., Eve, S., Jernot, J. P., Gomina, M., & Breard, J. (2009). Tensile deformation of a flax fiber. *Procedia Engineering*, *1*, 233–236.

Cheng, K., Winter, W. T., & Stipanovic, A. J. (2012). A modulated-TGA approach to the kinetics of lignocellulosic biomass pyrolysis/combustion. *Polymer Degradation and Stability*, *97*, 1606–1615.

Conrad, C. M. (1944). Determination of wax in cotton fiber: A new alcohol extraction method. *Industrial and Engineering Chemistry: Analytical Edition*, *16*, 745–748.

D'Almeida, J. R. M., Aquino, R. C. M. P., & Monteiro, S. N. (2006). Tensile mechanical properties, morphological aspects and chemical characterization of piassava (*Attala funifera*) fibers. *Composites: Part-A*, *37*, 1473–14739.

Das, M., & Chakrabarty, D. (2008). Thermogravimetric analysis and weathering study by water immersion of alkali-treated bamboo strips. *BioResource*, *3*, 1051–1062.

Di Blasi, C. (2002). Modeling intra- and extra-particle processes of wood fast pyrolysis. *American Institute of Chemical Engineers*, *48*, 2386–2397.

Dittenber, D. B., & Ganga Rao, H. V. S. (2012). Critical reviews of recent publications on use of natural composites in infrastructure. *Composites: Part-A*, *43*, 1419–1429.

Doree, C. (1950). *The methods of cellulose chemistry* (2nd ed.). London: Chapman and Hall.

Elenga, R. G., Dirras, G. F., Goma Maniongui, J., Djemia, P., & Biget, M. P. (2009). On the microstructure and physical properties of untreated raffia textilis fiber. *Composites: Part-A*, *40*, 418–422.

Faruk, O., Bledzkia, A. K., Finkb, H., & Sain, M. (2012). Biocomposites reinforced with natural fibers 2000–2010. *Progress in Polymer Science*, *37*, 1552–1596.

Fernando Pacheco-Torgal, & Jalali, S. (2011). Cementitious building materials reinforced with vegetable fibres: A review. *Construction and Building Materials*, *25*, 575–581.

Hejazi, S. M., Sheikhzadeh, M., Abtahi, S. M., & Zadhoush, A. (2012). A simple review of soil reinforcement by using natural and synthetic fibers. *Construction and Building Materials*, *30*, 100–116.

Helbert, W., Sugiyma, J., Ishihara, M., & Yamanaka, S. (1997). Characterization of native crystalline cellulose in the cell walls of *Oomy cota*. *Journal of Biotechnology*, *57*, 29–37.

Ho, M., Wang, H., Lee, J., Ho, C., Lau, K., Leng, J., et al. (2012). Critical factors on manufacturing processes of natural fibre composites. *Composites: Part-B*, *43*, 3549–3562.

Jawaid, M., & Abdul Khalil, H. P. S. (2011). Cellulosic/synthetic fibre reinforced polymer hybrid composites: A review. *Carbohydrate Polymers*, *86*, 1–18.

Jayaramudu, J., Guduri, B. R., & Varada Rajulu, A. (2010). Characterization of new natural cellulosic fabric *Grewia tilifolia*. *Carbohydrate Polymers*, *79*, 847–851.

Jeya, C., & Anuratha, C. V. (2010). *Cissus quadrangularis* stem alleviates insulin resistance, oxidative injury and fatty liver-disease in rats fed high fat plus fructose diet. *Food and Chemical Toxicology*, *48*, 2021–2029.

Khan, M. A., & Drzal, L. T. (2004). Characterization of 2-hydroxyethyl methacrylate (HEMA)-treated jute surface cured by UV radiation. *Journal of Adhesion Science and Technology*, *18*, 381–393.

Kiruthika, A. V., & Veluraja, K. (2009). Experimental studies on the physico-chemical properties of banana fibre from various varieties. *Fibers and Polymers*, *10*, 193–199.

Koronis, G., Silva, A., & Fontul, M. (2013). Green composites: A review of adequate materials for automotive applications. *Composites: Part-B*, *44*, 120–127.

Ku, H., Wang, H., Pattarachaiyakoop, N., & Trada, M. (2011). A review on the tensile properties of natural fiber reinforced polymer composites. *Composites: Part-B*, *42*, 856–873.

Kulkarni, A. G., Satyanarayana, K. G., & Rohatgi, P. K. (1983). Mechanical properties of banana fibers (Musa Sepientum). *Journal of Materials Science*, *18*, 2290–2296.

Mallika, J., & Shyamala Devi, C. S. (2006). Gastroprotective action of *Cissus quadrangularis* extract against NSAID induced gastric ulcer: Role of pro inflammatory cytokines and oxidative damage. *Chemico-Biological Interactions*, *161*, 262–270.

Mantia, F. P. L., & Morreale, M. (2011). Green composites: A brief review. *Composites: Part-A*, *42*, 579–588.

Mariana de Paula Ferreira, Nishijima, C. M., Seito, L. N., Dokkedal, A. L., Monica, L. F., Stasi, L. C. D., et al. (2008). Gastroprotective effect of *Cissus sicyoides* (Vitaceae): Involvement of microcirculation, endogenous sulfhydryl's and nitric oxide. *Journal of Ethnopharmacology*, *117*, 170–174.

Mohanty, A. K., Misra, M., & Hinrichsen, G. (2000). Biofibers, biodegradable polymers and biocomposites: An overview. *Macromolecular Materials and Engineering*, *276–277*, 1–24.

Morvan, C., Jauneau, A., Flaman, A., Millet, J., & Demarty, M. (1990). Degradation of flax polysaccharides with purified endo-polygalacturonase. *Carbohydrate Polymers*, *13*, 149–163.

O'Brien, T. P., Feder, N., & McCull, M. E. (1964). Polychromatic staining of plant cell walls by toludine blue – O. *Protoplasma*, *59*, 364–373.

Pearl, I. A. (1967). *The chemistry of lignin*. New York: Marcel Dekker (Chapter 4).

Perry, D. R. (1975). *Identification of textile materials* (7th ed.). London: The Textile Institute, Manara Printing Services.

Reddy, N., & Yang, Y. (2005). Structure and properties of high quality natural cellulose fibers from cornstalks. *Polymer*, *46*, 5494–5500.

Reddy, N., & Yang, Y. (2008). Characterizing natural cellulose fibers from velvet leaf (Abutilon Theophrasti) stems. *Bioresource Technology*, *99*, 2449–2454.

Sapsrithong, T., Kaewprem, W., Tongumpai, S., Nusuetrong, P., & Meksuriyen, D. (2012). *Cissus quadrangularis* ethanol extract up regulates superoxide dismutase, glutathione peroxidase and endothelial nitric oxide synthase expression in hydrogen peroxide-injured human ECV304 cells. *Journal of Ethnopharmacology*, *143*, 664–672.

Saravanakumar, S. S., Kumaravel, A., Nagarajan, T., Sudhakar, P., & Baskaran, R. (2013). Characterization of a novel natural cellulosic fiber from *Prosopis juliflora* bark. *Carbohydrate Polymers*, *92*, 1928–1933.

Sass, J. E. (1940). *Elements of botanical micro technique* (1st ed.). New York: McGraw Hill Book Co.

Sathishkumar, T. P., Navaneetha krishnan, P., & Shankar, S. (2012). Tensile and flexural properties of snake grass natural fiber reinforced isophthallic polyester composites. *Composites Science and Technology*, *72*, 1183–1190.

Satyanarayana, K. G., Sukumaran, K., Mukherjee, R. S., Pavithran, C., & Pillai, S. G. K. (1990). Natural fibre-polymer composites. *Cement and Concrete Composites*, *12*, 117–136.

Segal, L., Creely, J. J., Martin, A. E. J., & Conrad, C. M. (1959). An empirical method for estimating the degree of crystallinity of native cellulose using X-ray diffractometer. *Journal of Textile Research*, *29*, 786–794.

Sreenivasan, V. S., Somasundaram, S., Ravindran, D., Manikandan, V., & Narayanasamy, R. (2011). Microstructural, physico-chemical and mechanical characterization of *Sansevieria cylindrica* fibres – An exploratory investigation. *Materials and Design*, *32*, 453–461.

Yao, F., Wu, Q., Lei, Y., Guo, W., & Xu, Y. (2008). Thermal decomposition kinetics of natural fibers: Activation energy with dynamic thermo gravimetric analysis. *Polymer Degradation and Stability*, *93*, 90–98.

Zhbankov, R. G., Firsov, S. P., Buslov, D. K., Nikonenko, N. A., Marchewka, M. K., & Ratajczak, H. (2002). Structural physico-chemistry of cellulose macro molecules. Vibrational spectra and structures of cellulose. *Journal of Molecular Structure*, *614*, 117–125.

Zhong, B. Z., Ong, T., & Whong, W. Z. (1997). Studies on the relationship between treatment condition and micronucleus induction in V79 cells exposed to silica and glass fibers. *Mutation Research*, *391*, 111–116.